TISSUE ENGINEERING: Part A
Volume 23, Numbers 17 and 18, 2017

DOI: 10.1089/ten.tea.2016.0523

termis
Tissue Engineering
& Regenerative Medicine
International Society

SPECIAL FOCUS: STRATEGIC DIRECTIONS IN MUSCULOSKELETAL TISSUE ENGINEERING*

Skeletal Myoblast-Seeded Vascularized Tissue Scaffolds in the Treatment of a Large Volumetric Muscle Defect in the Rat Biceps Femoris Muscle

Mon-Tzu Li, PhD,[1,2] Marissa A. Ruehle, BS,[1,2] Hazel Y. Stevens, BS,[1] Nick Servies, BS,[1] Nick J. Willett, PhD,[1–3] Sukhita Karthikeyakannan, BS,[1] Gordon L. Warren, PhD,[4] Robert E. Guldberg, PhD,[1] and Laxminarayanan Krishnan, MBBS, PhD[1]

High velocity impact injuries can often result in loss of large skeletal muscle mass, creating defects devoid of matrix, cells, and vasculature. Functional regeneration within these regions of large volumetric muscle loss (VML) continues to be a significant clinical challenge. Large cell-seeded, space-filling tissue-engineered constructs that may augment regeneration require adequate vascularization to maintain cell viability. However, the long-term effect of improved vascularization and the effect of addition of myoblasts to vascularized constructs have not been determined in large VMLs. Here, our objective was to create a new VML model, consisting of a full-thickness, single muscle defect, in the rat biceps femoris muscle, and evaluate the ability of myoblast-seeded vascularized collagen hydrogel constructs to augment VML regeneration. Adipose-derived microvessels were cultured with or without myoblasts to form vascular networks within collagen constructs. In the animal model, the VML injury was created in the left hind limb, and treated with the harvested autograft itself, constructs with microvessel fragments (MVF) only, constructs with microvessels and myoblasts (MVF+Myoblasts), or left empty. We evaluated the formation of vascular networks *in vitro* by light microscopy, and the capacity of vascularized constructs to augment early revascularization and muscle regeneration in the VML using perfusion angiography and creatine kinase activity, respectively. Myoblasts (Pax7+) were able to differentiate into myotubes (sarcomeric myosin MF20+) *in vitro*. The MVF+Myoblast group showed longer and more branched microvascular networks than the MVF group *in vitro*, but showed similar overall defect site vascular volumes at 2 weeks postimplantation by microcomputed tomography angiography. However, a larger number of small-diameter vessels were observed in the vascularized construct-treated groups. Yet, both vascularized implant groups showed primarily fibrotic tissue with adipose infiltration, poor maintenance of tissue volume within the VML, and little muscle regeneration. These data suggest that while vascularization may play an important supportive role, other factors besides adequate vascularity may determine the fate of regenerating volumetric muscle defects.

Keywords: vascularized constructs, muscle regeneration, volumetric muscle loss

Introduction

Penetrating soft-tissue wounds are the most prevalent combat extremity injuries[1] and often involve extensive loss of skeletal muscle, also known as volumetric muscle loss (VML). This soft tissue trauma can result in edema, inflammation, a compromised vascular supply, and soft tissue necrosis at the injury site.[2] Loss of a large section of the muscle to injury or debridement results in a large space devoid of tissue, including blood vessels and stem cells. Coverage of the wound with a vascularized muscle flap can increase blood flow to the injured region and reduce the likelihood of infection but donor tissue availability can be limiting.[3] Even when treated, VML injuries are associated with poor long-term outcomes, including functional disability and pain.[4,5] No definitive regenerative therapy exists for large VML, and muscle flaps or

[1]Georgia Institute of Technology, Petit Institute for Bioengineering and Biosciences, Atlanta, Georgia.
[2]Department of Biomedical Engineering, Emory University, Atlanta, Georgia.
[3]Department of Orthopaedics, Atlanta Veteran's Affairs Medical Center, Decatur, Georgia.
[4]Department of Physical Therapy, Georgia State University, Atlanta, Georgia.

*This article is part of a special focus issue on Strategic Directions in Musculoskeletal Tissue Engineering. Additional articles can be found in Tissue Engineering Part A, volume 23, numbers 15–16 and Tissue Engineering Part B, number 4.

transpositions provide some cosmetic but little or no functional benefits.[6,7] Tissue-engineered strategies that offer repair and regeneration alternatives to limit loss of limb function have received significant attention in the last decade.[8]

Satellite cells are precursor cells existing in the adult muscles adjacent to muscle fibers.[9] These cells, expressing the transcriptional factor Pax7, are critical to muscle regeneration postinjury, and their conditional depletion has shown impaired regeneration in animal models.[10,11] Minced muscle autografts have been transplanted into a VML and show appreciable muscle regeneration within 4 weeks; these grafts may reflect a high regenerative potential in skeletal muscles.[12,13] Therapeutic use of cultured satellite cells, that is, myoblasts, has been hampered by their reduced regenerative capacity compared to satellite cells.[14,15] Yet, they remain a natural choice for engineered regenerative approaches to treat these large muscle defects by replacement of the lost tissue volume using cell-seeded scaffolds, since expansion of myoblasts from the primary satellite cell population *in vivo* or *in vitro* is an essential intermediate step in muscle regeneration. Furthermore, the size of space-filling scaffolds needed to fill large volumetric muscle defects mandates adequate attention to vascularization and nutrient/waste transport to prevent poor maintenance of delivered cells.[16] Indeed, coculture of cells, including myoblasts and endothelial cells, in tissue-engineered scaffolds has been previously reported to increase vascularity in smaller constructs implanted in the abdominal wall.[17]

Recent research into the use of vascularized constructs in mouse abdominal wall full-thickness defects showed benefits of early vascularization for graft survival and eventual functional integration with the skeletal muscle.[17,18] However, assembly of complex microvascular networks from endothelial and smooth muscle or similar cells requires an extended period of culture *in vitro*. A promising strategy to create vascularized constructs is the use of adipose-derived microvascular fragments.[19] These microvascular fragments undergo sprouting angiogenesis *in vitro*, are amenable to control of orientation,[19–24] and *in vivo* produce perfusion-capable blood vessels within a week of implantation, followed by further remodeling.[22,25–27] Recently, freshly isolated microvessel fragments, suspended in collagen hydrogels, were transplanted into a VML in the tibialis anterior (TA) muscle of the rat and showed higher vessel density in the defect site compared to acellular collagen gels or single cell containing scaffolds at 2 weeks postsurgery, although long-term muscle regeneration was not examined.[28]

Cultured microvascular fragments sacrifice the advantage of immediate transplantation, but the formation of nascent networks *in vitro* can facilitate rapid inosculation with host vessels[25,29] and may be pivotal to survival of large cell-seeded scaffolds. While microvascular fragments have been implanted both subcutaneously and in a VML with successful inosculation with host vessels, it is unclear whether vascularization is indeed a roadblock for effective muscle regeneration in VML. Thus, our *objective* was to determine the effects of a vascularized construct, with myoblasts, on the early revascularization and long-term muscle regeneration in a VML defect. We developed a large VML in the rat biceps femoris muscle to circumvent perceived disadvantages of existing models ranging from small size to VML defects with multi-muscle or multi-tissue injury in the evaluation of potential regenerative therapeutics.[8] In this study, we *hypothesized* that treatment of VML defects with vascularized tissue-engineered constructs, with or without myoblasts, would first lead to early vascularization and perfusion within the muscle defects, and subsequently result in improved muscle regeneration.

Materials and Methods

Myoblast isolation

Myoblasts were isolated from GFP-transgenic Sprague Dawley rats. Briefly, the soleus muscle, chosen for its high satellite cell density, was isolated from each leg, weighed, and placed in a small volume of sterile phosphate-buffered saline (PBS). The tissue was washed in sterile PBS and placed into 0.2% collagenase XI (6 mL for every two muscles, C9407; Sigma, St. Louis, MO). The muscle tissue was minced manually using two sterile razor blades for 5 min and transferred into a 15-mL conical tube. The tube was incubated in a 37°C water bath for 60 min, mixing once halfway through the incubation. Collagenase was then removed by centrifugation, and the homogenate pellet was suspended and incubated in dispase (2.4 U/mL, 6 mL for every two muscles; STEMCELL Technologies, Vancouver, CA) at 37°C for 45 min. The dispase was aspirated after centrifugation, and the pelleted cells were suspended in prewarmed myoblast growth media consisting of F10 (Thermo Fisher), 20% fetal bovine serum (Atlanta Biologicals, Lawrenceville, GA), 1% penicillin/streptomycin (Thermo Fisher), and 2.5 ng/mL bFGF (G-5071; Promega, Madison, WI). The cell suspension was then passed through a 100-μm filter (Steriflip; EMD Millipore-Sigma, St. Louis, MO) and preplated for 30 min on an uncoated dish to obtain a myoblast-enriched cell population in the supernatant. The supernatant was transferred to collagen-coated flasks and myoblasts were expanded for use between passages 3 and 4. All animal tissue harvest and implant-related procedures were reviewed and approved by the IACUC, Georgia Institute of Technology.

Microvessel isolation

Epididymal fat was isolated from Sprague Dawley rats as described earlier.[19,23,25] Twenty-nine animals were used for harvest of adipose tissue. Briefly, the isolated adipose tissue was washed and manually minced. The fat was subjected to limited digestion with lot-tested collagenase (2 mg/mL of fat, clostridial collagenase Ty I; Worthington Biochemical, Lakewood, NJ), after which vessels smaller than 500 microns and larger than 20 microns were isolated through appropriately sized nylon filters (Small Parts Brand, Amazon Business). The microvessels were then suspended in collagen solution (3 mg/mL, 20,000 microvessels/mL $\pm 10^6$ myoblasts/mL) and kept on ice until further use.

Vascularized constructs

To match the size of the vascularized constructs to the defect size and to minimize damage due to handling of the constructs during implantation and suturing to muscle tissue, gels were formed around a perforated electrospun polycaprolactone (PCL) membrane[30] suspended in a six-well plate between a two-part circular mold (Fig. 1A). A custom-machined Teflon mold, sterilized by autoclaving, was assembled in a well of a sterile six-well plate to create a smaller 15-mm-diameter well, across which the perforated PCL

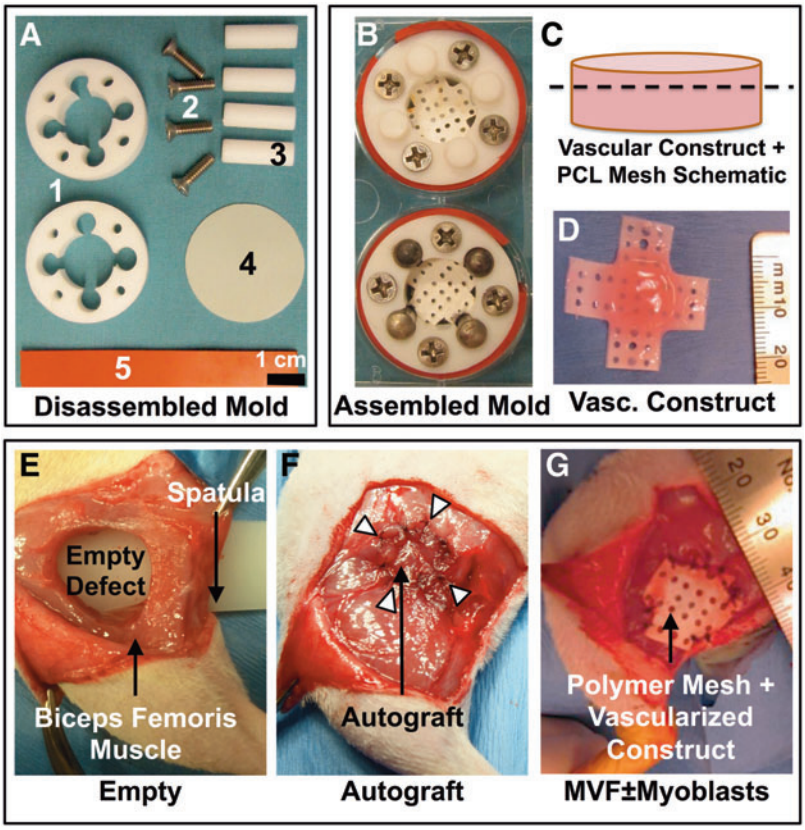

FIG. 1. Custom culture molds and volumetric muscle loss (VML) model in the rat biceps femoris muscle. **(A)** Components of the custom Teflon mold used to create vascularized constructs within individual wells of a six-well tissue culture plate, including 1—top and bottom Teflon rings between which the perforated polycaprolactone (PCL) membrane is suspended, 2—screws holding the PCL membrane stretched between the two Teflon rings, 3—the removable occluders (plastic or metal dowels) that are in place during gel formation and removed immediately to leave behind additional space to allow media circulation, 4—thin silicone membrane forming the bottom of the chamber to prevent leakage between the well base and the Teflon rings, and 5—thick silicone membrane wrapped around the Teflon mold to ensure a tight fit against the side and bottom of the well to prevent collagen solution leakage. **(B)** Fully assembled chamber mold with collagen gel formed around the perforated PCL mesh as shown in the schematic and photograph. **(C, D)** Schematic and photograph of vascularized collagen construct polymerized across the perforations in the PCL mesh (*dotted line*). **(E)** Creation of a 12-mm-diameter VML in the rat biceps femoris muscle. Plastic spatula placed underneath the biceps femoris muscle prevents injury to underlying tissues during creation of the VML. An untreated empty defect is pictured. **(F)** An autograft is sutured back into the defect immediately after harvest. **(G)** The vascularized collagen construct is sutured in place into the defect with excess PCL membrane trimmed away. This technique of suturing through the collagen gel and PCL membrane protects the collagen gel from damage during implantation. Color images available online at www.liebertpub.com/tea

membrane was stretched (Fig. 1A, B). A custom-cut silicone membrane was positioned at the base of the well, and a silicone strip was stretched around the mold to effectively provide a tight seal around the mold within the culture well. This step is essential to prevent the leakage of collagen solution around the mold (Fig. 1C). Removable dowels (metal or Teflon) were used to occlude regions around the central circular 15 mm opening during polymerization of the collagen solution. Approximately 2 mL of collagen solution with microvessels ± myoblasts was added slowly into these wells across the perforated mesh to ensure that collagen solution covered the mesh completely. The collagen solution was polymerized at 37°C for ~45 min, the four dowel occluders were then removed to allow space for media around the constructs, and constructs were cultured *in vitro* in 2–2.5 mL serum-free media,[24,31] for 4 days before implantation.

Characterization of myoblasts and vascularized constructs in vitro

Myoblasts were plated on eight-well chamber slides (4000 cells per 0.8 cm^2 well of eight-well chamber slides- LabTek II, Nunc, Thermo Fisher) and cultured in either myoblast growth media as described above or differentiation media consisting of DMEM (Thermo Fisher), 2% horse serum (Sigma) for 3–7 days, and fixed in 4% formaldehyde in PBS (paraformaldehyde; Sigma). Fixed cells were permeabilized with 0.2% Triton X-100 in PBS, washed copiously in PBS, blocked (1% w/v bovine serum albumin, 10% donkey serum, 0.3 M glycine, 0.1% Tween 20), and stained overnight with primary antibodies to Pax-7 (1:100; Abcam) and sarcomeric myosin (MF20; Developmental Studies Hybridoma Bank). Fluorescently labeled secondary antibodies were then used to

identify myoblasts. Fluorescent signals from GFP+ cells are quenched after formalin fixation and did not interfere with MF20 staining.[32] The potential of culture-expanded myoblasts to differentiate into muscle cells was also examined by MF20 antibody staining, as above, which recognizes myosin in terminally differentiated muscle cells.

One vascularized construct containing microvessels from Lewis rats and myoblasts (MVF+Myoblasts) was cultured in the custom chamber molds for 4 days, as described above for viability analysis with a live/dead assay (Thermo Fisher), corresponding to the time of implantation. Image-based quantification of cell viability was carried out in ImageJ. Ten random images from the construct were processed by binarization of the images (two channels: live—green, dead—red) and automated object identification, followed by size filtering of the object areas to remove any particles smaller than the typical cell size (below 5 pixels considered noise) and the large multicellular microvessels (above 200 pixels). Both the number of objects and the area occupied were determined and expressed as a percentage of live cells (green) compared to the total (green + red). Similar collagen constructs with MVF only and MVF+Myoblasts (GFP+) were cultured in 48-well plates (250 μL, four samples each) for 4 days, fixed, stained *en bloc* with GS1-lectin (Vector Labs, Burlingame, CA), and imaged. Maximum intensity z-projections of confocal images (10× objective; Zeiss) acquired from a random location per sample for each of the four samples per vascularized group were generated. The images were skeletonized in ImageJ and the total network lengths and the number of branches were compared between the two groups as metrics of microvascular growth and network formation, respectively.

VML defect creation

Unilateral biceps femoris muscle defects were created in 13-week-old female Sprague Dawley rats. The biceps femoris muscle was separated by blunt dissection from the more medial semimembranosus and semitendinosus muscles. A plastic spatula was inserted between the biceps femoris and the other knee flexor muscles to provide a stable surface for a 12 mm biopsy punch to push against and to guard the underlying structures while creating the full-thickness cylindrical muscle defect (Fig. 1E–G). The defect was left empty, treated by suturing the cut muscle piece back in place approximately as harvested (autograft), treated with a microvessel fragment (MVF) construct, or treated with a microvessel fragment construct with myoblasts (MVF+Myoblasts). Overall, 24 animals were assigned to the vascularization study at 2 weeks, four animals each were used for histological analysis at 2 and 8 weeks postinjury (one additional animal for autograft histology at 4 weeks), and 27 animals were used for terminal evaluations of the total creatine kinase (CK) activity. The unoperated right legs were used as controls for biochemical assays.

Microcomputed tomography angiography

At 2 weeks postinjury, 24 animals ($n = 5$–7 as per each of the four treatment groups) were euthanized and perfused with a contrast agent for microcomputed tomography (micro-CT) angiography. The technique has been previously described in detail.[33–35] Briefly, physiological saline (0.9% NaCl) containing 0.4% papaverine hydrochloride (Sigma-Aldrich) was perfused through the vasculature via a transcardiac catheter in the ascending aorta, to clear the blood vessels. This was followed by fixation with 10% neutral buffered formalin and a subsequent flush with physiological saline. The vasculature was finally injected with a lead chromate-based radiopaque contrast agent (Microfil MV-22, 2:1 mix with diluent; Flow Tech, Carver, MA). Animals were stored at 4°C overnight to allow for polymerization of the contrast agent. The biceps femoris was excised, and the defect region (marked with sutures) was isolated. For contralateral control legs, a 12-mm biopsy punch was used to remove a similarly sized piece of uninjured biceps femoris muscle.

Excised samples were further fixed for 48 h in normal buffered formalin and then stored in PBS. Samples were scanned in the micro-CT (vivaCT 40; Scanco Medical) at 21 μm voxel size. All scans were performed with an applied electrical potential of 55 kVp and a current of 109 μA. The volume of interest (VOI) consisted of a cylindrical volume of 14.7 mm in diameter that spanned the full thickness of the biceps femoris and included the entire sample disc harvested. A global threshold was applied for segmentation of vasculature, and a Gaussian low-pass filter was used to suppress noise ($\sigma = 0.8$, support = 1). Analysis scripts within the native Scanco software suite were used to estimate the total vascular volume and vessel diameter distribution histograms (incremental 21 μm bins).[36] The vascularity parameters were compared across groups to determine the extent of vascular perfusion produced by the vascularized or cell-seeded constructs.

CK activity

At 8 weeks, 27 animals were euthanized ($n = 6$–8 per group), and the original defect site was harvested using a 12-mm biopsy punch, as during creation of the VML defect. The harvested tissue was weighed (wet weight), flash-frozen in liquid nitrogen, and stored at −80°C until homogenization. For the CK assay, muscle tissues were removed from −80°C, minced, and hand homogenized (Duall™ tissue grinders; Kimble-Chase Kontes, Vineland, NJ) in 100 mM potassium phosphate buffer (pH 7.4) used at a ratio of 400 μL of buffer for every 50 mg of tissue. Homogenates were frozen and stored at −80°C until analysis. After centrifugation at 10,000 *g* for 15 min, supernatants were assayed for CK activity using an assay kit (MAK116; Sigma-Aldrich) following the manufacturer's instructions. CK activity was normalized to wet weight of the harvested tissue.

Histology

One random muscle sample per group per time point was paraffin embedded and 5-um-thick transverse sections were taken from the middle of the muscle defect. Sections were stained with hematoxylin and eosin and Masson's trichrome as described earlier.[37,38] GFP immunohistochemistry (ab290; Abcam) was performed to identify myoblasts in the MVF+Myoblast implant group, stained with the nuclear stain DAPI, and examined on a fluorescent microscope (Zeiss Axio Observer).

Statistical analyses

Statistical differences in microvascular network parameters between MVF-only and MVF+Myoblast groups were

examined using Welch's *t*-test ($\alpha = 0.05$). One-way analysis of variance (ANOVA) ($\alpha = 0.05$) with *post-hoc* tests for pairwise differences or its nonparametric equivalent (Kruskal–Wallis rank test, with Dunn's *post-hoc* comparisons) was used in quantitative comparisons of vascular volume. The differences in distribution of vessels in different diameter bins (21 μm incremental bins, 0 to ≤231 μm) across the four injury (treatment) groups were analyzed by two-way ANOVA. Similarly, the differences in CK values between the injured (treated, left) legs and the control legs were also analyzed by two-way repeated measures-ANOVA (RM-ANOVA). Data are reported as mean ± SD or SEM and are explicitly mentioned for each comparison along with the sample numbers (*n*).

Results

In vitro *growth of myoblasts and microvessels*

Tissue culture flask-expanded myoblasts cultured on eight-well chamber slides stained strongly for the marker Pax7 both immediately after seeding (Fig. 2A) and after 1 week of growth in myoblast growth medium (Fig. 2B), qualitatively supporting the incorporation of a relatively pure population of myoblasts at the time of incorporation into the vascularized scaffolds. These cells were successfully differentiated into myocytes *in vitro* by growth in differentiation media, as evidenced by positive staining for sarcomeric myosin (MF20) and areas of apparent fusion of multiple cells, giving the appearance of myotube formation (Fig. 2C).

A live/dead assay on a construct, similar to ones used for implantation, revealed high viability of microvessels and the coseeded myoblasts. The microvascular fragments appeared predominantly viable (green, calcein) from a single plane confocal image (Fig. 3A, B) and were excluded from quantification based on size (area) cutoff filters on binarized images (Fig. 3C, D). Quantification of 10 random images of the stained construct showed 68% ± 4.7% of cells to be viable representing 79% ± 3.8% of the total area occupied.

Microvessel networks appeared to be greater in the MVF+Myoblast constructs than the MVF-only constructs (Fig. 4A, B). Network analysis ($n = 4$ per group, Fig. 4C) showed a more branched network with higher branch numbers ($p = 0.0003$) in the MVF+Myoblast constructs compared to MVF-only constructs. In agreement, the MVF+Myoblast constructs had a higher mean network length ($p = 0.0003$) compared to MVF-only constructs (Fig. 4D).

Early vascularization in VML defects

The muscle samples harvested after contrast perfusion were imaged to identify the radiopaque vascular networks. Three-dimensional reconstructions of micro-CT image stacks revealed striking qualitative differences between the empty defects, which had a comparatively sparse vessel network, and the three treatment groups, which showed a larger number of smaller vessels (Fig. 5A, representative images). The MVF+Myoblast (MVF+My) group appeared to have the densest networks composed of predominantly smaller vessels. The overall vascular volumes between the injured groups were not different at 2 weeks (Fig. 5B), irrespective of the treatment they received (Kruskal–Wallis one-way ANOVA). However, the diameter distribution of the vessels in the injured groups showed a peak in small-diameter vessels in all groups, consistent with the expected angiogenic response, especially in the microvascular-treated groups (Fig. 5C). Since the microvessels supplemented in the vascularized constructs were primarily small length and small-diameter vessels (7–25 μm),[22,28] we performed further statistical analysis on vessels with diameters ≤231 μm (two-way ANOVA for differences between treatment groups within each diameter bin, $\alpha = 0.05$, Holm–Sidak's *post-hoc* multiple comparisons). A significantly higher number of smaller vessels, between 42 and 147 μm, were seen in the microvessel-treated groups compared to Empty or Autograft groups (Fig. 5D). Since significant differences in diameter distribution were observed only within the smaller diameter bins, vascular volumes contributed by these smaller vessels were also compared in the distribution where a peak in smaller vessels was observed. For vessels ≤105 μm in diameter, a higher volume was seen in the MVF group compared to the Empty defects ($p = 0.04$, Kruskal–Wallis test, Dunn's *post hoc*). A similar comparison of all smaller vessels ≤231 μm in diameter (Fig. 5E), corresponding to the vessels in Figure 5D, revealed a similar trend in averages, without significant differences ($p = 0.06$, Kruskal–Wallis test, Dunn's *post hoc*). Qualitative histology of perfused muscle defects at 2 weeks showed well-perfused large- and small-diameter vessels in all injured groups along with a presence of abundant cellular infiltration (Fig. 5F–I).

CK activity

We used a two-way RM-ANOVA (Bonferroni's *post-hoc* multiple comparisons) to test for differences in CK activity. There was no significant interaction of treatment or leg ($p = 0.086$), or main effect of treatment. As expected, there

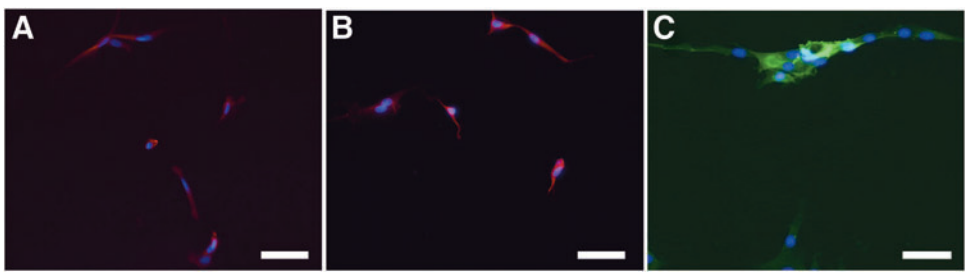

FIG. 2. Characterization of myoblasts *in vitro*. **(A)** Myoblasts cultured on slides show predominantly Pax7-positive cells on the first day of culture (*red*—Pax7, nuclei—*blue*, DAPI). **(B)** Similarly, cultured myoblasts in growth media at day 7 staining for Pax7. **(C)** Myoblasts cultured in myogenic differentiation media for 72 h stain positive for MF 20 (*green*) and show early signs of myotube formation. Scale bar: 50 μm. Color images available online at www.liebertpub.com/tea

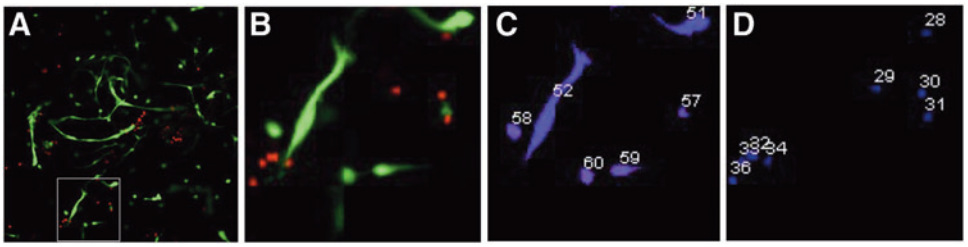

FIG. 3. Viability of vascularized constructs *in vitro*. **(A)** A single plane image acquired by confocal microscopy after viability analysis (*green*—live, *red*—dead). Microvessels are predominantly stained green and are viable. The majority of single cells are also viable (68%) based on image quantification. **(B)** Zoomed in view of area highlighted in **(A)**. **(C)** A representative image highlighting the selection of live objects corresponding to **(B)**. Large object #52 not included in quantitative analysis after filter implementation. **(D)** Representative image of dead object selection. Note that these images are of cultures generated within custom molds as described in Figure 1. Color images available online at www.liebertpub.com/tea

was a significant main effect of leg ($p < 0.0001$) with the mean activity of the injured legs being lower (MVF: 0.45 ± 0.036, MVF+My: 0.52 ± 0.049, Empty: 0.68 ± 0.043, Autograft: 0.67 ± 0.048; Mean ± SEM) than that of the uninjured legs (Fig. 6).

Qualitative histology

In agreement with the CK data, qualitative histology at both 2 weeks (Fig. 5F–I) and 8 weeks (Fig. 7A–D) did not show muscle regeneration in the muscle defects treated with MVF±Myoblast constructs. Few implanted GFP-myoblasts were identified at the defect margin at 2 and 8 weeks (Fig. 7E–G). In Mason's trichrome stained images of autograft-treated VML at 2 and 4 weeks after implantation, varying levels of fibrous tissue infiltration were evident in the muscle tissue (stained blue-green in Fig. 7H, I).

Discussion

Two critical questions in engineering large tissue constructs and developing VML replacement therapies are as follows: (1) Is there an effect of improvement in early vascularization on long-term regeneration? (2) What is the effect of adding tissue-specific progenitor cells to these vascularization strategies? To address these questions, we investigated regeneration within a challenging 12-mm-diameter, full-thickness defect model in the rat biceps femoris muscle by use of vascularized constructs with and without the inclusion of myoblasts. At 2 weeks postimplantation, the VMLs treated with microvascular constructs showed a higher number of small-diameter vessels

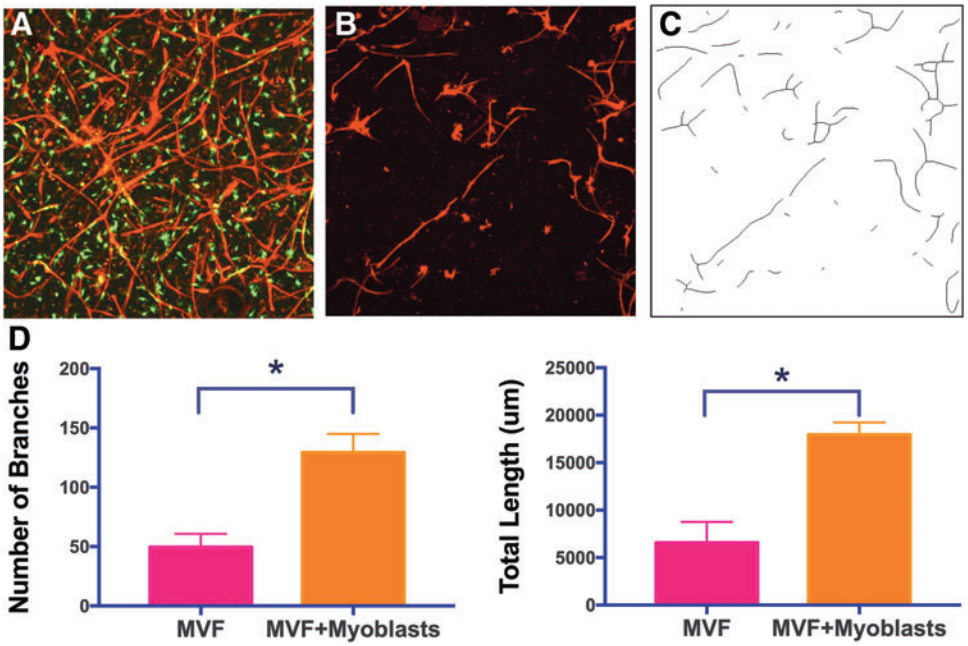

FIG. 4. Microvascular network growth analysis *in vitro*. **(A)** Maximum intensity z projection of MVF+Myoblast constructs at day 4 of culture (*red*—GS1-lectin-stained MVF, *green*—GFP+Myoblasts). **(B)** MVF-only constructs, illustrating less network formation without myoblast addition as in **(A)**. **(C)** Representative skeletonization image used in microvascular network analysis corresponding to the GS1-lectin-stained images in **(B)**. **(D)** Quantification of total branch numbers and network lengths between MVF and MVF+Myoblast constructs (mean ± SD, $n = 4$ per group, *indicates statistical significance, $p < 0.05$). Note that these images are of cultures generated in standard 48-well tissue culture plates. MVF, microvessel fragments. Color images available online at www.liebertpub.com/tea

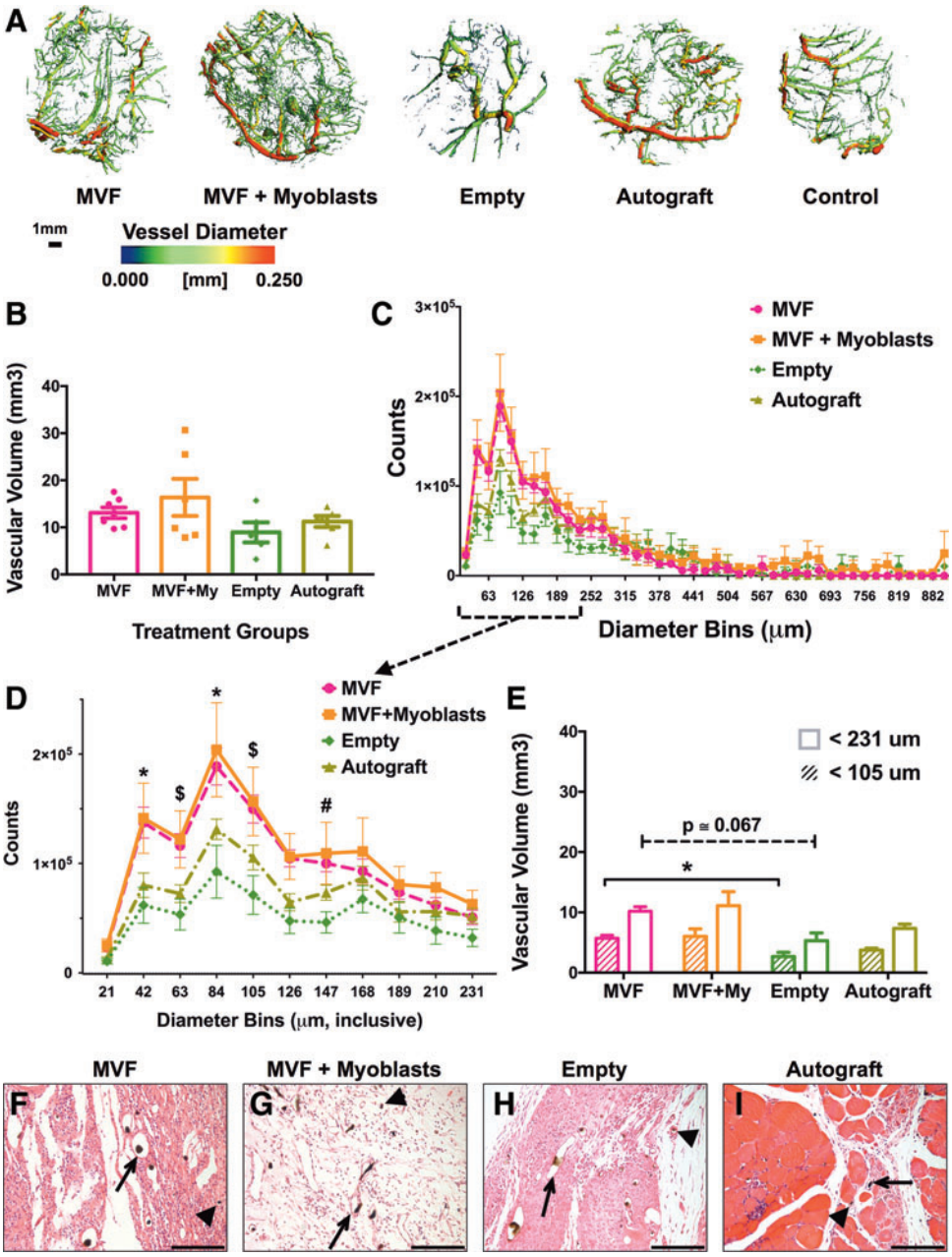

FIG. 5. Vascular volume in microvessel-treated biceps femoris. **(A)** Representative images of the vasculature in each group show that the MVF ± Myoblast groups have comparable vascular volume to the autograft group. Vessels are colored according to their respective diameters. **(B)** At 2 weeks postinjury, overall vascular volumes were not significantly different between groups (*$p < 0.05$, mean ± SEM, $n = 5–7$ for injured groups). **(C)** Histogram of vessel diameter distribution across 21-μm-sized diameter bins, showing a peak at the smaller diameter range. **(D)** Subset of the histogram data of vessels ≤231 μm diameter. Notations for significant differences ($p < 0.05$, two-way analysis of variance [ANOVA] for simple effects within diameter bins): *MVF, MVF+My versus Autograft, Empty, $^{\$}$MVF, MVF+My versus Empty, $^{\#}$MVF+My versus Empty defects. **(E)** Vascular volumes reflective of the two diameter cutoffs analyzed (*$p < 0.05$, mean ± SEM, $n = 5–7$ for injured groups), and **(F–I)** eosin and hematoxylin-stained sections of injured muscles after 2 weeks of healing (20× images) show large (*arrow*) and small (*arrow head*) microvessels perfused with Microfil, which appears as *black pigment* in the lumen. It must be noted that Microfil can be dislodged from the slide during staining. Scale bar: 150 μm. Color images available online at www.liebertpub.com/tea

compared to untreated empty defects and autograft-treated defects. Although the overall vascular volume between the treatment groups was not significantly different as hypothesized, the vascular volume contributed by the smaller vessels was higher in the MVF group compared to the empty defect. These observations suggest that the implanted microvessels indeed participated in angiogenesis, were perfusion capable at 2 weeks, and may have allowed adequate gas and nutrient exchange within the implanted constructs.

However, contrary to our hypothesis, neither the MVF nor MVF+Myoblast constructs resulted in muscle regeneration 8 weeks postinjury. The muscle CK enzyme levels

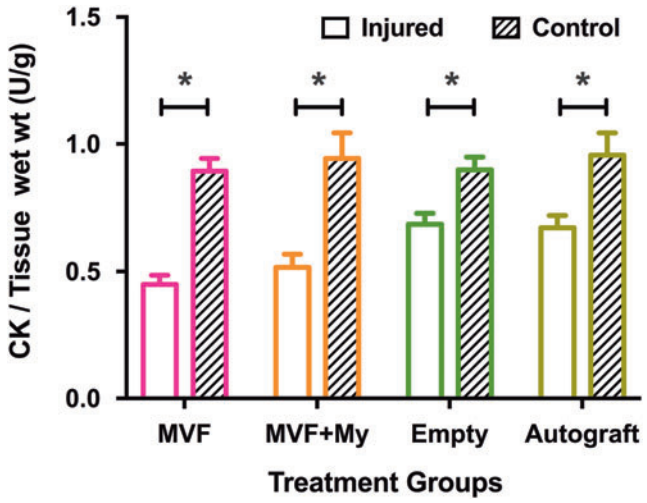

FIG. 6. Creatine kinase (CK) activity 8 weeks postinjury. Comparisons of mean CK activity per gram muscle wet mass between and within treatment groups (two-way repeated measures-ANOVA, Bonferroni's *post-hoc* multiple comparison). Mean CK levels of the injured legs (*left*) were lower than the corresponding contralateral controls (*right leg*) within the treatment groups. (*MVF: $p < 0.0001$, MVF+My: $p < 0.0001$, Empty: $p = 0.0304$, Autograft: $p = 0.0006$, $n = 6$–8 per group, mean ± SEM). Color images available online at www.liebertpub.com/tea

were lower in all injured groups signifying poor muscle regeneration. *In vitro* evaluations support both the successful expansion of myoblasts (Pax7+) from harvested satellite cells and their ability to differentiate to myocytes (MF20+). Furthermore, appreciable cell survival in large constructs after 4 days *in vitro* and the presence of a nascent microvascular network that can support rapid inosculation with the host circulation[25] suggest that the myoblasts were viable and differentiation capable, with the potential for early blood perfusion at the time of implantation. The observed viability of 68%, although lower than typically expected, is encouraging after 4 days of *in vitro* culture in a large construct of this size. We have previously reported comparable viability (52–85%) in larger microvessel-seeded collagen constructs (~3 mL) with circulating media, depending on the mode of circulation and region of the gel, after 10 days of culture.[39] Using bioluminescence tracking, we have also previously reported viability of about 60% and lower in cell-seeded alginate or agarose scaffolds of 150 μL volume after 7 days of subcutaneous implantation *in vivo*.[40] While implanted myoblasts can regenerate muscle fibers and integrate with host tissue,[41] their regenerative capacity may be significantly reduced compared to the use of freshly isolated satellite cells due to a reduction in proliferation and increase in differentiation, thus limiting the numbers of available progenitors.[15,42] In addition, the regeneration within the large VML defects used here may have been influenced by the local factors such as the inflammatory environment[43] or the presence of fibroblasts.[44]

The inflammatory response postmuscle injury has been well studied and important roles have been ascribed to macrophage polarization.[45–47] In this study, microvessels and myoblasts were implanted allogeneically into Sprague Dawley rats. Although not investigated in this study, collagen scaffolds are known to have inherently low immunogenicity[48] and may modulate and even lower the immune response.[49] The presence of fibrous tissue infiltration in the microvessel containing groups and the autograft tissue, along with the high cellular infiltrate, suggests that inflammation may be one of the contributing factors impeding regeneration. This is supported by impaired myoblast differentiation (myotube) in the presence of fibroblasts at least *in vitro*.[44] Importantly, this study supports the presence of a higher number of smaller perfused vessels as expected, likely derived from the implanted microvessels. Interestingly, although the total volumes were smaller compared to injured legs, an increase in the vascular volumes of the contralateral control legs in the groups receiving microvessels was also noticed suggesting possible systemic effects.

Engineered therapeutics for muscle replacement or vascularization have been evaluated in smaller abdominal wall defects (3 mm^2) in mice[17,18] and a relatively larger 6-mm-diameter full-thickness TA muscle defect in rats.[28] Large VMLs, however, better model clinical scenarios of extensive muscle damage and complex tissue injuries.[8] Our model of VML in the rat biceps femoris muscle was intended to provide a larger and more challenging environment for evaluation of therapeutics. This relatively superficial flat muscle, ranging from 2 to 5 mm in thickness, is distinctly separate from the surrounding muscles, easily accessible, and allows for the creation of a 12-mm-diameter full-thickness defect weighing 0.35 ± 0.04 g (mean ± SD, immediately after VML creation), without damaging the adjacent muscles or neurovascular bundles. Importantly, the size and volumes of engineered constructs needed for repair reflect the challenging size of this VML model, and highlight its applicability as a preclinical evaluation platform for engineered therapeutics. While the previously reported TA defect (~0.120 g or lower) was packed with a 0.4 mL collagen hydrogel made in a 48-well culture plate,[28] the constructs we used were significantly larger (five times greater in volume, ~2 mL solution), representing the larger scaffolds that could be screened in this model for therapeutic efficiency. The fact that the empty defect does not show any muscle regeneration endogenously supports the challenging nature of this VML model.

Vessel diameter distribution data as discussed earlier suggest the availability of more small-diameter vessels in the microvessel-treated groups to participate in blood perfusion, with a higher vascular volume in the MVF-treated group. Between the vascularized groups, the inclusion of myoblasts did not significantly improve vascular volumes measured at 2 weeks. This was contrary to expectations given our *in vitro* results and the known paracrine stimulatory effect of myoblasts on angiogenic growth.[50] The explanation may lie in the timing of our vascular volume measurements in relation to the microvascular network remodeling *in vivo*, reflecting possible differences in the mechanical environment[22–24] and the process of network maturation and adaptation to form hierarchical microvascular beds.[26] In addition, the short preculture period in this study that allowed the formation of nascent angiogenic sprouts and networks may have led to rapid inosculation,[25,51] resulting in fewer differences within well-vascularized structures due to angioadaptation such as the metabolic environment.[52–54] Recent evidence also suggests dependence of muscle capillary density on the muscle fiber size.[55] Hence, associated factors that can influence vessel adaptation must also be simultaneously considered to explain the role of a competent microcirculation in regeneration.

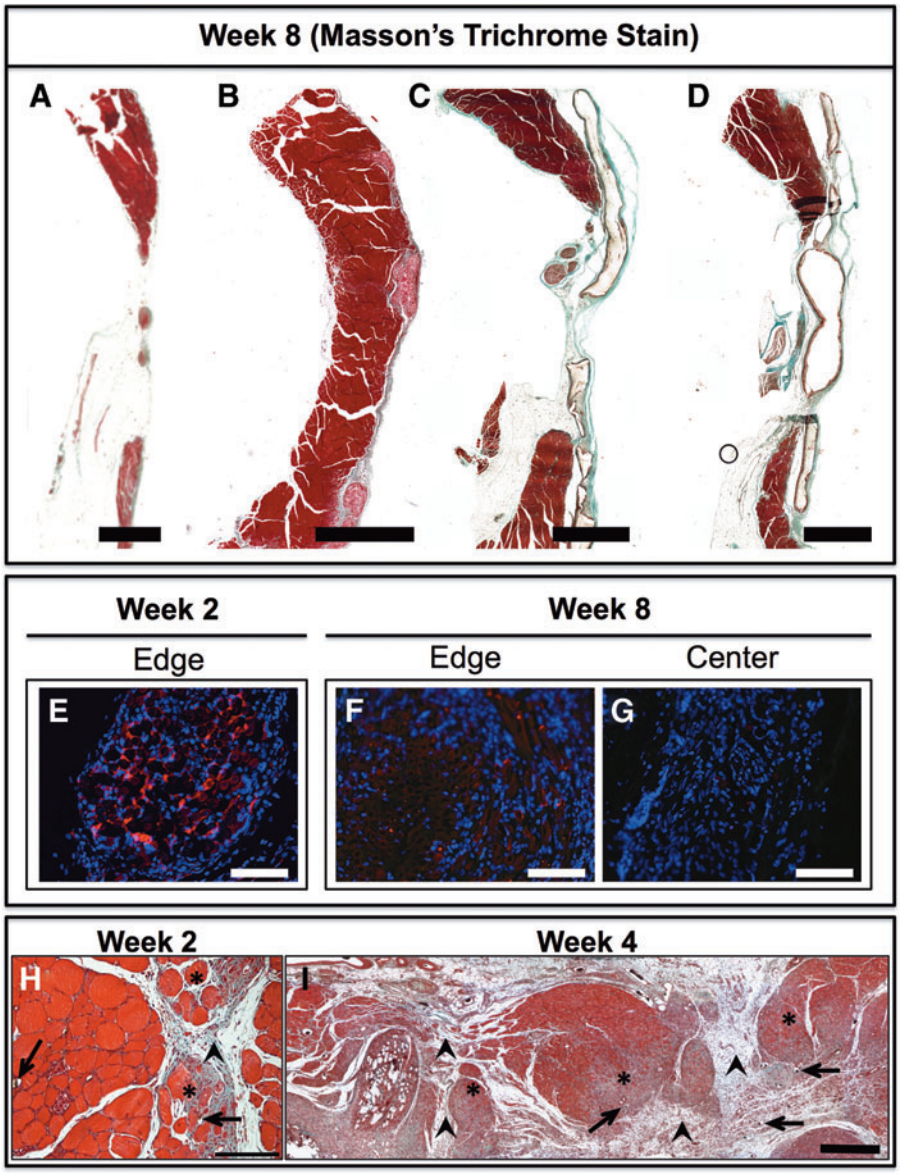

FIG. 7. Qualitative histology. Transverse section of biceps femoris muscle 8 weeks postinjury, stained with Masson's trichrome, showing empty defect **(A)**, autograft **(B)**, MVF **(C)**, and MVF+Myoblast **(D)** group 8 weeks after injury. Implanted collagen constructs appear replaced by loose fibrous tissue similar to empty defects (*blue-green*) and autograft tissue appeared to be maintained. Transverse sections of MVF+Myoblast-treated biceps femoris 2 weeks **(E)** and 8 weeks **(F)** after injury showing surviving myoblasts (IHC: *red*—GFP myoblasts, *blue*—nuclei) at the defect margin but not at the defect center **(G)**. 4× Mosaic scale bar: 2 mm **(A–D)**, 10× scale bar: 100 μm **(E–G)**. **(H–I)** Masson's trichrome-stained section of an autograft-treated sample at 2 weeks **(H)** and 4 weeks **(I)** postimplantation showing fibrous tissue (*arrowhead*) in the defect around the autograft, and showing fibrous infiltration of muscle tissue (*). These regions appear highly vascularized as evidenced by the Microfil-perfused vessels (*arrows*) seen in these areas. Scale bar: 150 μm **(H)** and 500 μm **(I)**. Color images available online at www.liebertpub.com/tea

Literature evidence, including observations in fracture healing studies, suggests that an adequate vascular response is essential in successful regeneration.[16,56] To the best of our knowledge, only the previous study using microvascular constructs to treat volumetric muscle defects demonstrated an increase in local vascular density in the first 2 weeks when freshly harvested microvessels were implanted into the muscle defect but did not comprehensively characterize muscle regeneration.[8,28] The vessel diameter distribution data support the existence of more numerous smaller diameter vessels capable of perfusion in the microvessel-treated groups. However, postmortem intracardiac angiography may not accurately reflect the dynamic perfusion status of the remodeling nascent microvascular network tissue or the phenomenon of capillary recruitment.[57] The lack of differences in overall vascular volume between treatment groups may also be a result of the time point selected or environment-dependent changes in vessel networks, where a failure in healing progression may have led to vessel network remodeling.[53] Thus, the lack of vascular angiography data at an earlier time point (<2 weeks) is a possible limitation of this study. However, the larger question was on the influence of vascularization support strategies, if any, on muscle regeneration as similar vascularization and cell-seeding approaches are being investigated as regenerative strategies.[17,18,28] Whether the angiogenic response is the limiting factor for muscle regeneration in large VMLs is yet unclear, but our study suggests that addition of vessels and progenitor cells may not be sufficient to induce any significant improvement in muscle regeneration over untreated defects, even in terms of retention of implant volume in large clinically relevant volumetric muscle defects. Another limitation of this study is the lack of measurement of muscle functional capacity (e.g., strength). Instead, qualitative histological observations suggesting variable fibrous tissue infiltration of autograft and a lack of retention of implanted vascular constructs and a quantitative evaluation of the levels of the enzyme CK, which is ubiquitously expressed in skeletal muscle, provided information on the therapeutic efficacy of the vascularization strategies in this study.

Acellular scaffolds used to treat VMLs have shown functional improvement,[58] but limited muscle regeneration

compared to muscle autografts.[43] The use of myogenic cell-seeded and vascularized scaffolds used in this study represents attempts to recreate the benefits of autografts. Quiescent satellite cells undergo asymmetric division on activation (e.g., post-injury) to generate stem cells that may return to quiescence and replenish the satellite cell population as well as myoblasts that, after further symmetric division (expansion) and fusion, ultimately form myofibers.[42] The size of engineered tissues needed to repair large VMLs necessitates culture expansion, but there is growing consensus that freshly isolated satellite cells offer the best regenerative potential and even short periods of culture expansion of these cells, now myoblasts, hamper their regenerative capacity.[15,42] Taken together with our data, it is clear that the replacement of extracellular matrix (ECM) alone, myogenic cells, and vasculatures is insufficient to induce muscle regeneration. In addition to the cellular component, other critical factors to be considered in future works may include innervation, mechanical loading, and a compatible volume retaining ECM structure capable of adequate load transfer to growing cells. While stem cells prefer an appropriate substrate elastic modulus (8–17 kPa) to promote myogenic differentiation,[59] the collagen hydrogel used here has a lower elastic modulus (1.53 kPa).[23,60] We, and others, have also shown that collagen concentration of the hydrogels (and hence the elastic modulus) also influences microvascular growth and morphology.[61,62] Hence, in this initial study, we elected to evaluate collagen hydrogel-based scaffolds that have previously shown robust microvascular network formation *in vivo*.[22,27] We believe that our data reinforce the need to consider the role of appropriate substrates in developing tissue-engineered replacement therapies for muscle regeneration.

Conclusions

In this study, we have evaluated the effects of vascularized constructs with and without myoblasts on the augmentation of vascularization of the biceps femoris muscle defect and its regeneration, after a VML injury. The vascularized constructs provided a higher number of perfusion-capable smaller diameter vessels compared to Empty and Autograft-treated defects, and hence would be expected to be competent in overcoming any perceived barriers in vascular support. Implanted myoblasts were also present at the edge of the muscle defects at 2 and 8 weeks after delivery. These strategies did not result in regeneration of muscle within the defect space as assessed by tissue CK content. While further studies are needed to better understand the appropriate environment and scaffolds conducive to muscle regeneration, this study indicated that the recovery of vascular supply in the defect space alone, even with added progenitor cells, was insufficient to augment muscle regeneration in large volumetric muscle defects.

Acknowledgments

The authors thank Dr. Dong. G J and Dr. Li. K F, Shandong Sports University, Jinan, China, for their assistance with CK assays. This work was supported by the Army, Navy, NIH, Air Force, VA, and Health Affairs to support the AFIRM II effort, under Award No. W81XWH-14-2-0003. Opinions, interpretations, conclusions, and recommendations are those of the authors and are not necessarily endorsed by the Department of Defense. This work was also supported by an NIH Cell and Tissue Engineering training grant.

Disclosure Statement

No competing financial interests exist.

References

1. Owens, B.D., Kragh, J.F., Jr., Macaitis, J., Svoboda, S.J., and Wenke, J.C. Characterization of extremity wounds in Operation Iraqi Freedom and Operation Enduring Freedom. J Orthop Trauma **21,** 254, 2007.
2. Borrelli, J., Jr. Management of soft tissue injuries associated with tibial plateau fractures. J Knee Surg **27,** 5, 2014.
3. Park, J.J., Campbell, K.A., Mercuri, J.J., and Tejwani, N.C. Updates in the management of orthopedic soft-tissue injuries associated with lower extremity trauma. Am J Orthop **41,** E27, 2012.
4. Matsuoka, T., Yoshioka, T., Tanaka, H., Ninomiya, N., Oda, J., Sugimoto, H., and Yokota, J. Long-term physical outcome of patients who suffered crush syndrome after the 1995 Hanshin-Awaji earthquake: prognostic indicators in retrospect. J Trauma **52,** 33, 2002.
5. MacKenzie, E.J., Bosse, M.J., Pollak, A.N., Webb, L.X., Swiontkowski, M.F., Kellam, J.F., Smith, D.G., Sanders, R.W., Jones, A.L., Starr, A.J., McAndrew, M.P., Patterson, B.M., Burgess, A.R., and Castillo, R.C. Long-term persistence of disability following severe lower-limb trauma. Results of a seven-year follow-up. J Bone Joint Surg Am **87,** 1801, 2005.
6. Rossiter, N.D., Higgins, T.F., and Pallister, I. (ii) The mangled extremity: limb salvage versus amputation. Orthop Trauma **28,** 137, 2014.
7. Corona, B.T., Rivera, J.C., Owens, J.G., Wenke, J.C., and Rathbone, C.R. Volumetric muscle loss leads to permanent disability following extremity trauma. J Rehabil Res Dev **52,** 785, 2015.
8. Willett, N.J., Krishnan, L., Li, M.T., Guldberg, R.E., and Warren, G.L. Guidelines for models of skeletal muscle injury and therapeutic assessment. Cells Tissues Organs **202,** 214, 2016.
9. Mauro, A. Satellite cell of skeletal muscle fibers. J Biophys Biochem Cytol **9,** 493, 1961.
10. Murphy, M.M., Lawson, J.A., Mathew, S.J., Hutcheson, D.A., and Kardon, G. Satellite cells, connective tissue fibroblasts and their interactions are crucial for muscle regeneration. Development **138,** 3625, 2011.
11. Sambasivan, R., Yao, R., Kissenpfennig, A., Van Wittenberghe, L., Paldi, A., Gayraud-Morel, B., Guenou, H., Malissen, B., Tajbakhsh, S., and Galy, A. Pax7-expressing satellite cells are indispensable for adult skeletal muscle regeneration. Development **138,** 3647, 2011.
12. Bierinx, A.S., and Sebille, A. Mouse sectioned muscle regenerates following auto-grafting with muscle fragments: a new muscle precursor cells transfer? Neurosci Lett **431,** 211, 2008.
13. Carlson, B.M., and Gutmann, E. Development of contractile properties of minced muscle regenerates in the rat. Exp Neurol **36,** 239, 1972.
14. Tedesco, F.S., Dellavalle, A., Diaz-Manera, J., Messina, G., and Cossu, G. Repairing skeletal muscle: regenerative potential of skeletal muscle stem cells. J Clin Invest **120,** 11, 2010.
15. Montarras, D., Morgan, J., Collins, C., Relaix, F., Zaffran, S., Cumano, A., Partridge, T., and Buckingham, M. Direct isolation of satellite cells for skeletal muscle regeneration. Science **309,** 2064, 2005.

16. Auger, F.A., Gibot, L., and Lacroix, D. The pivotal role of vascularization in tissue engineering. Annu Rev Biomed Eng **15,** 177, 2013.
17. Levenberg, S., Rouwkema, J., Macdonald, M., Garfein, E.S., Kohane, D.S., Darland, D.C., Marini, R., van Blitterswijk, C.A., Mulligan, R.C., D'Amore, P.A., and Langer, R. Engineering vascularized skeletal muscle tissue. Nat Biotechnol **23,** 879, 2005.
18. Koffler, J., Kaufman-Francis, K., Shandalov, Y., Egozi, D., Pavlov, D.A., Landesberg, A., and Levenberg, S. Improved vascular organization enhances functional integration of engineered skeletal muscle grafts. Proc Natl Acad Sci U S A **108,** 14789, 2011.
19. Hoying, J.B., Boswell, C.A., and Williams, S.K. Angiogenic potential of microvessel fragments established in three-dimensional collagen gels. In Vitro Cell Dev Biol Anim **32,** 409, 1996.
20. Stabenfeldt, S.E., Gourley, M., Krishnan, L., Hoying, J.B., and Barker, T.H. Engineering fibrin polymers through engagement of alternative polymerization mechanisms. Biomaterials **33,** 535, 2012.
21. Laschke, M.W., and Menger, M.D. Adipose tissue-derived microvascular fragments: natural vascularization units for regenerative medicine. Trends Biotechnol **33,** 442, 2015.
22. Chang, C.C., Krishnan, L., Nunes, S.S., Church, K.H., Edgar, L.T., Boland, E.D., Weiss, J.A., Williams, S.K., and Hoying, J.B. Determinants of microvascular network topologies in implanted neovasculatures. Arterioscler Thromb Vasc Biol **32,** 5, 2012.
23. Krishnan, L., Hoying, J.B., Nguyen, H., Song, H., and Weiss, J.A. Interaction of angiogenic microvessels with the extracellular matrix. Am J Physiol Heart Circ Physiol **293,** H3650, 2007.
24. Krishnan, L., Underwood, C.J., Maas, S., Ellis, B.J., Kode, T.C., Hoying, J.B., and Weiss, J.A. Effect of mechanical boundary conditions on orientation of angiogenic microvessels. Cardiovasc Res **78,** 324, 2008.
25. Shepherd, B.R., Chen, H.Y., Smith, C.M., Gruionu, G., Williams, S.K., and Hoying, J.B. Rapid perfusion and network remodeling in a microvascular construct after implantation. Arterioscler Thromb Vasc Biol **24,** 898, 2004.
26. Nunes, S.S., Greer, K.A., Stiening, C.M., Chen, H.Y., Kidd, K.R., Schwartz, M.A., Sullivan, C.J., Rekapally, H., and Hoying, J.B. Implanted microvessels progress through distinct neovascularization phenotypes. Microvasc Res **79,** 10, 2010.
27. Nunes, S.S., Krishnan, L., Gerard, C.S., Dale, J.R., Maddie, M.A., Benton, R.L., and Hoying, J.B. Angiogenic potential of microvessel fragments is independent of the tissue of origin and can be influenced by the cellular composition of the implants. Microcirculation **17,** 557, 2010.
28. Pilia, M., McDaniel, J.S., Guda, T., Chen, X.K., Rhoads, R.P., Allen, R.E., Corona, B.T., and Rathbone, C.R. Transplantation and perfusion of microvascular fragments in a rodent model of volumetric muscle loss injury. Eur Cells Mater **28,** 11, 2014.
29. Gibot, L., Galbraith, T., Huot, J., and Auger, F.A. A preexisting microvascular network benefits in vivo revascularization of a microvascularized tissue-engineered skin substitute. Tissue Eng Part A **16,** 3199, 2010.
30. Krishnan, L., Priddy, L.B., Esancy, C., Li, M.T., Stevens, H.Y., Jiang, X., Tran, L., Rowe, D.W., and Guldberg, R.E. Hydrogel-based delivery of rhBMP-2 improves healing of large bone defects compared with autograft. Clin Orthop Relat Res **473,** 2885, 2015.
31. Bottenstein, J.E., and Sato, G.H. Growth of a rat neuroblastoma cell line in serum-free supplemented medium. Proc Natl Acad Sci U S A **76,** 514, 1979.
32. Schnell, U., Dijk, F., Sjollema, K.A., and Giepmans, B.N. Immunolabeling artifacts and the need for live-cell imaging. Nat Methods **9,** 152, 2012.
33. Boerckel, J.D., Kolambkar, Y.M., Dupont, K.M., Uhrig, B.A., Phelps, E.A., Stevens, H.Y., Garcia, A.J., and Guldberg, R.E. Effects of protein dose and delivery system on BMP-mediated bone regeneration. Biomaterials **32,** 5241, 2011.
34. Duvall, C.L., Taylor, W.R., Weiss, D., and Guldberg, R.E. Quantitative microcomputed tomography analysis of collateral vessel development after ischemic injury. Am J Physiol Heart Circ Physiol **287,** H302, 2004.
35. Uhrig, B.A., Boerckel, J.D., Willett, N.J., Li, M.T., Huebsch, N., and Guldberg, R.E. Recovery from hind limb ischemia enhances rhBMP-2-mediated segmental bone defect repair in a rat composite injury model. Bone **55,** 410, 2013.
36. Boerckel, J.D., Uhrig, B.A., Willett, N.J., Huebsch, N., and Guldberg, R.E. Mechanical regulation of vascular growth and tissue regeneration in vivo. Proc Natl Acad Sci U S A **108,** E674, 2011.
37. Willett, N.J., Li, M.T., Uhrig, B.A., Boerckel, J.D., Huebsch, N., Lundgren, T.L., Warren, G.L., and Guldberg, R.E. Attenuated human bone morphogenetic protein-2-mediated bone regeneration in a rat model of composite bone and muscle injury. Tissue Eng Part C Methods **19,** 316, 2013.
38. Li, M.T., Willett, N.J., Uhrig, B.A., Guldberg, R.E., and Warren, G.L. Functional analysis of limb recovery following autograft treatment of volumetric muscle loss in the quadriceps femoris. J Biomech **47,** 2013, 2014.
39. Chang, C.C., Nunes, S.S., Sibole, S.C., Krishnan, L., Williams, S.K., Weiss, J.A., and Hoying, J.B. Angiogenesis in a microvascular construct for transplantation depends on the method of chamber circulation. Tissue Eng Part A **16,** 795, 2010.
40. Allen, A.B., Gazit, Z., Su, S., Stevens, H.Y., and Guldberg, R.E. In vivo bioluminescent tracking of mesenchymal stem cells within large hydrogel constructs. Tissue Eng Part C Methods **20,** 806, 2014.
41. Borselli, C., Cezar, C.A., Shvartsman, D., Vandenburgh, H.H., and Mooney, D.J. The role of multifunctional delivery scaffold in the ability of cultured myoblasts to promote muscle regeneration. Biomaterials **32,** 8905, 2011.
42. Shadrach, J.L., and Wagers, A.J. Stem cells for skeletal muscle repair. Philos Trans R Soc Lond B Biol Sci **366,** 2297, 2011.
43. Aurora, A., Corona, B.T., and Walters, T.J. A porcine urinary bladder matrix does not recapitulate the spatiotemporal macrophage response of muscle regeneration after volumetric muscle loss injury. Cells Tissues Organs **202,** 189, 2015.
44. Rao, N., Evans, S., Stewart, D., Spencer, K.H., Sheikh, F., Hui, E.E., and Christman, K.L. Fibroblasts influence muscle progenitor differentiation and alignment in contact independent and dependent manners in organized co-culture devices. Biomed Microdevices **15,** 161, 2013.
45. Badylak, S.F., Valentin, J.E., Ravindra, A.K., McCabe, G.P., and Stewart-Akers, A.M. Macrophage phenotype as a determinant of biologic scaffold remodeling. Tissue Eng Part A **14,** 1835, 2008.
46. Tidball, J.G. Inflammatory processes in muscle injury and repair. Am J Physiol Regul Integr Comp Physiol **288,** R345, 2005.
47. Villalta, S.A., Nguyen, H.X., Deng, B., Gotoh, T., and Tidball, J.G. Shifts in macrophage phenotypes and macro-

phage competition for arginine metabolism affect the severity of muscle pathology in muscular dystrophy. Hum Mol Genet **18,** 482, 2009.
48. Abou Neel, E.A., Bozec, L., Knowles, J.C., Syed, O., Mudera, V., Day, R., and Hyun, J.K. Collagen—emerging collagen based therapies hit the patient. Adv Drug Deliv Rev **65,** 429, 2013.
49. Yuan, T., Li, K., Guo, L., Fan, H., and Zhang, X. Modulation of immunological properties of allogeneic mesenchymal stem cells by collagen scaffolds in cartilage tissue engineering. J Biomed Mater Res Part A **98,** 332, 2011.
50. Rhoads, R.P., Johnson, R.M., Rathbone, C.R., Liu, X., Temm-Grove, C., Sheehan, S.M., Hoying, J.B., and Allen, R.E. Satellite cell-mediated angiogenesis in vitro coincides with a functional hypoxia-inducible factor pathway. Am J Physiol Cell Physiol **296,** C1321, 2009.
51. Laschke, M.W., Mussawy, H., Schuler, S., Kazakov, A., Rucker, M., Eglin, D., Alini, M., and Menger, M.D. Short-term cultivation of in situ prevascularized tissue constructs accelerates inosculation of their preformed microvascular networks after implantation into the host tissue. Tissue Eng Part A **17,** 841, 2011.
52. LeBlanc, A.J., Krishnan, L., Sullivan, C.J., Williams, S.K., and Hoying, J.B. Microvascular repair: post-angiogenesis vascular dynamics. Microcirculation **19,** 676, 2012.
53. Pries, A.R., Reglin, B., and Secomb, T.W. Remodeling of blood vessels: responses of diameter and wall thickness to hemodynamic and metabolic stimuli. Hypertension **46,** 725, 2005/10.
54. Pries, A.R., and Secomb, T.W. Origins of heterogeneity in tissue perfusion and metabolism. Cardiovasc Res **81,** 328, 2009.
55. Bosutti, A., Egginton, S., Barnouin, Y., Ganse, B., Rittweger, J., and Degens, H. Local capillary supply in muscle is not determined by local oxidative capacity. J Exp Biol **218,** 3377, 2015.
56. Krishnan, L., Willett, N.J., and Guldberg, R.E. Vascularization strategies for bone regeneration. Ann Biomed Eng **42,** 432, 2014.
57. Fry, B.C., Roy, T.K., and Secomb, T.W. Capillary recruitment in a theoretical model for blood flow regulation in heterogeneous microvessel networks. Physiol Rep **1,** e00050, 2013.
58. Aurora, A., Roe, J.L., Corona, B.T., and Walters, T.J. An acellular biologic scaffold does not regenerate appreciable de novo muscle tissue in rat models of volumetric muscle loss injury. Biomaterials **67,** 393, 2015.
59. Engler, A.J., Sen, S., Sweeney, H.L., and Discher, D.E. Matrix elasticity directs stem cell lineage specification. Cell **126,** 677, 2006.
60. Krishnan, L., Weiss, J.A., Wessman, M.D., and Hoying, J.B. Design and application of a test system for viscoelastic characterization of collagen gels. Tissue Eng **10,** 241, 2004.
61. Krishnan, L., Utzinger, U., Maas, S., Reese, S., Weiss, J.A., Williams, S.K., and Hoying, J.B. Extracellular matrix stiffness modulates microvascular morphology during early sprouting angiogenesis in vitro. Presented at the ASME 2009 Summer Bioengineering Conference, Lake Tahoe, CA. New York, 2009.
62. Edgar, L.T., Underwood, C.J., Guilkey, J.E., Hoying, J.B., and Weiss, J.A. Extracellular matrix density regulates the rate of neovessel growth and branching in sprouting angiogenesis. PLoS One **9,** e85178, 2014.

Address correspondence to:
Laxminarayanan Krishnan, MBBS, PhD
Georgia Institute of Technology
Petit Institute for Bioengineering and Biosciences
315 Ferst Drive
Atlanta, GA 30332-0363

E-mail: lkrishnan@gatech.edu

Robert E. Guldberg, PhD
Georgia Institute of Technology
Petit Institute for Bioengineering and Biosciences
315 Ferst Drive
Atlanta, GA 30332-0363

E-mail: robert.guldberg@me.gatech.edu

Received: November 30, 2016
Accepted: March 20, 2017
Online Publication Date: August 23, 2017